

Article

Thermodynamics of Regular Cosmological Black Holes with the de Sitter Interior

Irina Dymnikova^{1,2,*} and Michał Korpusik¹

¹ Department of Mathematics and Computer Science, University of Warmia and Mazury, Słoneczna 54, 10-710 Olsztyn, Poland; E-Mail: m.korpusik@matman.uwm.edu.pl

² A.F.Ioffe Physico-Technical Institute, Polytekhnicheskaya 26, 194021 St. Petersburg, Russia

* Author to whom correspondence should be addressed; E-Mail: irina@uwm.edu.pl; Tel.: +48-89-524-60-38; Fax: +48-89-524-60-89.

Received: 3 August 2011; in revised form: 14 November 2011 / Accepted: 16 November 2011 / Published: 28 November 2011

Abstract: We address the question of thermodynamics of regular cosmological spherically symmetric black holes with the de Sitter center. Space-time is asymptotically de Sitter as $r \rightarrow 0$ and as $r \rightarrow \infty$. A source term in the Einstein equations connects smoothly two de Sitter vacua with different values of cosmological constant: $8\pi GT_{\nu}^{\mu} = \Lambda\delta_{\nu}^{\mu}$ as $r \rightarrow 0$, $8\pi GT_{\nu}^{\mu} = \lambda\delta_{\nu}^{\mu}$ as $r \rightarrow \infty$ with $\lambda < \Lambda$. It represents an anisotropic vacuum dark fluid defined by symmetry of its stress-energy tensor which is invariant under the radial boosts. In the range of the mass parameter $M_{cr1} \leq M \leq M_{cr2}$ it describes a regular cosmological black hole. Space-time in this case has three horizons: a cosmological horizon r_c , a black hole horizon $r_b < r_c$, and an internal horizon $r_a < r_b$, which is the cosmological horizon for an observer in the internal R-region asymptotically de Sitter as $r \rightarrow 0$. We present the basic features of space-time geometry and the detailed analysis of thermodynamics of horizons using the Padmanabhan approach relevant for a multi-horizon space-time with a non-zero pressure. We find that in a certain range of parameters M and $q = \sqrt{\Lambda/\lambda}$ there exist a global temperature for an observer in the R-region between the black hole horizon r_b and cosmological horizon r_c . We show that a second-order phase transition occurs in the course of evaporation, where a specific heat is broken and a temperature achieves its maximal value. Thermodynamical preference for a final point of evaporation is thermodynamically stable double-horizon ($r_a = r_b$) remnant with the positive specific heat and zero temperature.

Keywords: space-time horizons; regular black hole; evaporation; black hole remnants

1. Introduction

In 1973 Four laws of black hole mechanics were formulated [1], and Bekenstein introduced a black hole entropy [2]. A year later Hawking found a quantum evaporation of a black hole [3,4] which gave the birth to thermodynamics of black holes [5–7] (for a review see [8]). In 1976 Gibbons and Hawking found that also cosmological horizon can radiate [9], and this gave rise to thermodynamics of horizons [10–18].

Astronomical observations testify that our universe is dominated at above 73 % of its density by a dark energy responsible for its accelerated expansion due to negative pressure, $p = w\rho$, $w < -1/3$ [19–25], with the best fit $w = -1$ [26–31] corresponding to a cosmological constant λ ([32] and references therein). This motivates study of cosmological black holes.

Studies of black hole thermodynamics in the de Sitter space are also important in the context of the quantum theory of gravity and of dark matter physics. Theoretical developments suggest the existence of a holographic duality between quantum gravity on de Sitter space and a certain Euclidean conformal field theory on its spacelike boundary, dS/CFT correspondence [33,34]. Black hole remnants are considered as a source of dark matter for more than two decades [35–39] (for a review see [40,41]), and are under search at the CERN LHC [42,43].

The basic problem concerning black hole remnants is which remnants (if any) leave from the Hawking evaporation. Generalized uncertainty principle requires the existence of a remnant of the Planck mass [38]. On the other hand, an evident symmetry or quantum number preventing complete evaporation is not found [44]. Another problem concerning the Planck mass remnant is that its entropy seems to be zero [38], although the second law of black hole thermodynamics requires $S = 4\pi r_h^2$ [5], and for a remnant the horizon radius $r_h \neq 0$. This question and its relation to the third law of thermodynamics will be discussed in Section 5.

Thermodynamics of black holes in the de Sitter space is in essence thermodynamics in a multi-horizon space-time. The Schwarzschild-de Sitter metric belongs to the class of space-time metrics

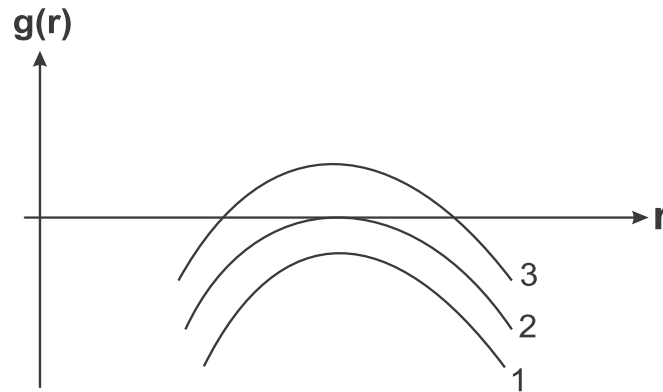
$$ds^2 = g(r)dt^2 - \frac{dr^2}{g(r)} - r^2 d\Omega^2 \quad (1)$$

The metric function is given by

$$g(r) = 1 - \frac{2GM}{r} - \frac{r^2}{l^2} \quad (2)$$

where M is the mass parameter and l is related to the background cosmological constant λ by $l^2 = 3/\lambda$. Basic features of a space-time described by (2) depend on the value of the quantity $D = 9M^2\lambda - 1$. For $D < 0$ it describes a Schwarzschild-de Sitter black hole with two horizons (curve 3 in Figure 1). The case of double horizon $D = 0$ corresponds to the Nariai solution (curve 2 in Figure 1), and for $D > 0$ the metric (4) is the Kantowski-Sachs metric describing an anisotropic homogeneous universe (curve 1 in Figure 1).

Figure 1. Metric function for the Schwarzschild-de Sitter space-time.



The Schwarzschild-de Sitter black hole emits the Hawking radiation from both horizons [9], but in general they are not in thermal equilibrium. The Gibbons-Hawking temperature on a horizon r_h with a surface gravity κ_h

$$kT_h = \frac{\hbar}{2\pi c} \kappa_h = \frac{\hbar}{4\pi c} |g'(r_h)| \tag{3}$$

corresponds to the periodicity of the Euclidean quantum field theory in the Euclidean time $t_E = it$. In the Kruskal coordinates introduced to avoid a singularity at the horizon, the Kruskal time

$$T_E = \frac{e^{\kappa r_*}}{\kappa} \sin(\kappa t_E); \quad r_* = \int \frac{dr}{g(r)} \tag{4}$$

is the periodic function of t_E with the period $\beta = 2\pi/\kappa$ related directly to the inverse quantum temperature of a horizon. In the case of two horizons it is impossible to obtain, by one transformation, regularity on both horizons, so that an observer would detect the mixture of radiations from horizons [9]. A common (global) temperature can be defined only in the case when the relation of surface gravities on horizons is the rational number [45,46]. The Kruskal extension of the metric (1) needs a separate coordinate patch for each horizon. For each patch the Kruskal extension takes the form $ds^2 = g_{b,c}(dt_{b,c}^2 - dr_{b,c}^2) - r^2 d\Omega^2$. The new and old time coordinates are related by $t'_{b,c} = e^{\mp \kappa_{b,c} r_*} \sinh(\kappa_{b,c} t)$. In the Euclidean time $t_E = it$ a minimal period appears as the lowest common multiple of $2\pi/\kappa_{b,c}$ when the ratio $\kappa_b/\kappa_c = n_b/n_c$ is a rational number (n_b, n_c are prime integers) [45,46]

$$\frac{\kappa_b}{\kappa_c} = \frac{n_b}{n_c} \tag{5}$$

From the minimal period $\beta = 2\pi n_b/\kappa_b = 2\pi n_c/\kappa_c$, one obtains a global temperature [45,46]

$$kT = \frac{\hbar}{c} \frac{1}{\beta} = \frac{\hbar}{2\pi c} \frac{(\kappa_b + \kappa_c)}{(n_b + n_c)} = \frac{\hbar}{2\pi c} \frac{\kappa_b}{n_b} = \frac{\hbar}{2\pi c} \frac{\kappa_c}{n_c} \tag{6}$$

Dynamical evolution of the Schwarzschild-de Sitter black hole is typically studied for two horizons separately. Teitelboim considered the Euclidean Schwarzschild-de Sitter geometry as an extremum of two different action principles. He analyzed evolution of a cosmological horizon with a black hole as a boundary, and evolution of a black hole with a cosmological horizon as a boundary, identifying a black hole mass M as a thermodynamical energy [16]. He found the tendency of growing the mass parameter M in the course of evaporation so that a black hole would evolve to the Nariai state. On the other

hand, applying the second law of thermodynamics for a manifold between the horizons, Aros found an opposite tendency—complete evaporation of a black hole [18], which agrees with the results obtained in [47,48].

Complete evaporation creates the problem clearly formulated by Aros [18]: In the Schwarzschild-de Sitter space-time the cosmological horizon is not observer-dependent as in the de Sitter space, but real horizon—due to presence of the black hole which breaks the global symmetries involving the radial direction. A serious doubt concerns a causal structure of space-time: the fate of energy radiated once a black hole disappears “leaving behind the de Sitter space with nothing beyond the cosmological horizon but the de Sitter space itself, so energy can not be hidden there” [18]. Complete evaporation would create one more serious problem—how to evaporate a singularity? [49].

The uncertainties concerning endpoint of evaporation are related to the problem of a unique definition of thermodynamical parameters for the case of two horizons. A general approach for defining thermodynamical variables was proposed by Padmanabhan [12–14]. He considered the spherically symmetric Einstein equations as the thermodynamical identity for the class of solutions described by the line element (1) which leads to the results confirmed by consideration of a canonical ensemble of space-time metrics from the class (1) at the constant temperature of the horizon determined by the periodicity of the Euclidean time in the Euclidean continuation of the Einstein action; the partition function for this ensemble calculated as the path integral sum [12], can be written as

$$Z(kT_h) = Z_0 \exp \left[\frac{1}{4} (4\pi r_h^2) - \frac{1}{kT_h} \left(\frac{|g'|}{g} \frac{r_h}{2} \right) \right] \propto \exp \left[S(r_h) - \frac{E(r_h)}{kT_h} \right] \quad (7)$$

which leads to the identification

$$S = \frac{1}{4} (4\pi r_h^2); \quad E = \frac{|g'|}{g} \frac{r_h}{2} = \frac{|g'|}{g} \left(\frac{A_h}{16\pi} \right)^{1/2} \quad (8)$$

where S is the entropy, E is the thermodynamical energy, g is value of the metric function on a horizon, g' is its derivative on a horizon, and A_h is the horizon area.

In this paper we apply the Padmanabhan approach to study thermodynamics of a regular cosmological black hole with three horizons, which differs from the Schwarzschild-de Sitter black hole in that a central singularity is replaced with a de Sitter vacuum core.

The idea of replacing a Schwarzschild singularity with a de Sitter vacuum goes back to 1965 papers by Sakharov [50] who considered $p = -\rho$ as the equation of state for superhigh density, and by Gliner who interpreted $p = -\rho$ as corresponding to a vacuum with a non-zero density and suggested that it could be a final state in a gravitational collapse [51]. In 1988 Poisson and Israel proposed to introduce a transitional layer of an uncertain depth where geometry can be self-regulatory and describable semiclassically by the Einstein equations with a source term representing vacuum polarization effects [52]. The regular black hole with the de Sitter vacuum interior was proposed first in 1990 [53] but was lucky to be published only in 1992 after awarding by the Gravity Research Foundation in 1991 [54].

Now situation looks as follows: A loop quantum gravity provides arguments in favor of a regular black hole [55,56]. Analyzing a Schwarzschild interior in frame of a minisuperspace model, Modesto found that the curvature invariant and the inverse volume operator have a finite spectrum inside a horizon [57]. The “renormalization group improving” approach based on the running Newton constant

($G = G(k)$, $k = k(r)$ in the spherically symmetric case) applied to the Schwarzschild space-time predicts an appearance of a smooth de Sitter core replacing a singularity [58]. The noncommutative geometry approach (for a review see [60], see also [61]) applied to the Schwarzschild black hole, leads to a regular de Sitter core at short distances from the origin [62]. Appearance of de Sitter core was found also for a cosmological noncommutative black hole of positive mass with the Gaussian density profile [63].

On the other hand, the Einstein equations admit the class of regular spherically symmetric solutions asymptotically de Sitter at both the origin and infinity [64–66]. It was found by investigation of typical features of spherically symmetric solutions to the Einstein equations. Such an approach is in essence model-independent; questions are addressed to equations (“what know equations”).

For this class of spherically symmetric solutions a source term connects smoothly two de Sitter vacua with different values of cosmological constant ($\Lambda\delta_k^i$ as $r \rightarrow 0$, $\lambda\delta_k^i$ as $r \rightarrow \infty$ with $\Lambda > \lambda$), and corresponds to anisotropic vacuum dark fluid [67] defined by symmetry of its stress-energy tensor. In a certain range of the mass parameter, $M_{cr1} \leq M \leq M_{cr2}$, a solution of this class describes a regular cosmological black hole with the de Sitter interior [68,69].

A smooth de Sitter-Schwarzschild transition has been described by the spherically symmetric Einstein equations with a source term satisfying [54]

$$T_t^t = T_r^r; \quad T_\theta^\theta = T_\phi^\phi \quad (9)$$

The equation of state, following from $T_{\nu;\mu}^\mu = 0$, is

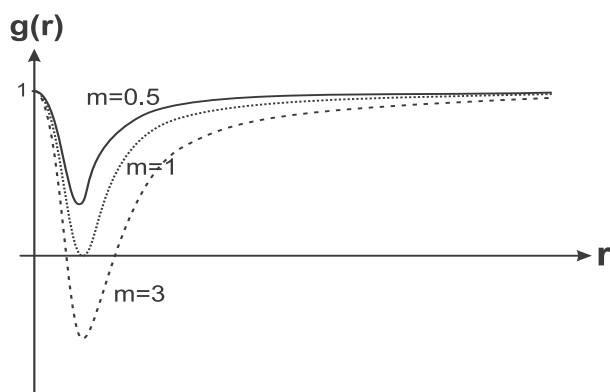
$$p_r = -\rho; \quad p_\perp = -\rho - \frac{r}{2}\rho' \quad (10)$$

where $\rho(r) = T_t^t$ is the energy density, $p_r(r) = -T_r^r$ is the radial pressure, and $p_\perp(r) = -T_\theta^\theta = -T_\phi^\phi$ is the tangential pressure for anisotropic perfect fluid.

A stress-energy tensor specified by (9) and satisfying the weak energy condition (non-zero density for any observer on a time-like curve) represents a spherically symmetric anisotropic (see (10)) vacuum fluid [54,64–67,70,71] whose symmetry is reduced as compared with the maximally symmetric de Sitter vacuum [72]. Vacuum with a reduced symmetry (for a review see [73–79]) provides a unified description of dark ingredients in the Universe by a vacuum dark fluid [67,71], which represents distributed vacuum dark energy by a time evolving and spatially inhomogeneous cosmological term [64], and compact objects with de Sitter vacuum interior: regular black holes and gravitational vacuum solitons G-lumps [65,67] which are regular gravitationally bound vacuum structures without horizons (dark particles or dark stars, dependently on a mass) [65,80,81]. Mass of a compact object is generically related to interior de Sitter vacuum and to breaking of space-time symmetry from the de Sitter group in the origin [65,77,79].

A regular spherically symmetric black hole with the de Sitter center is described by the metric (1). In the asymptotically flat case, the metric is asymptotically de Sitter for $r \rightarrow 0$ and asymptotically Schwarzschild for large r . It has two horizons which coincide for a certain mass M_{cr} corresponding to an extreme black hole [65,80]. Typical behavior of the metric function is shown in Figure 2. The parameter m refers to the mass M normalized to M_{cr} ($m < 1$ corresponds to G-lump).

Figure 2. Metric function for de Sitter-Schwarzschild space-time.



It evaporates from both horizons, and generic asymptotic behavior of the metric function $g(r)$ defines dynamics of evaporation. It involves a phase transition where a specific heat is broken and changes its sign. At the final stage a temperature vanishes on a double horizon [65,80,82]. A regular black hole leaves behind a thermodynamically stable remnant with the positive specific heat [84] (free of the existential problems).

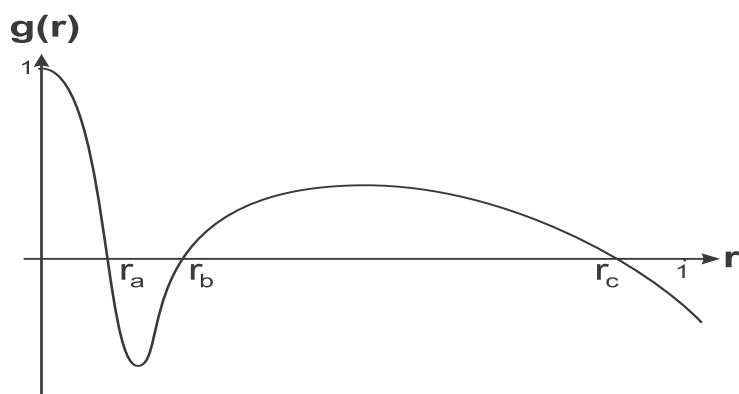
A regular cosmological black hole with the de Sitter center in place of a singularity ($g(r) \rightarrow 1 - \Lambda r^2/3$ as $r \rightarrow 0$) is described by the metric function [68]

$$g(r) = 1 - \frac{2G\mathcal{M}(r)}{r} - \frac{\lambda r^2}{3}; \quad \mathcal{M}(r) = 4\pi \int_0^r \rho(x)x^2 dx \tag{10}$$

whose asymptotics are the de Sitter metrics with λ as $r \rightarrow \infty$ and with $(\Lambda + \lambda)$ as $r \rightarrow 0$.

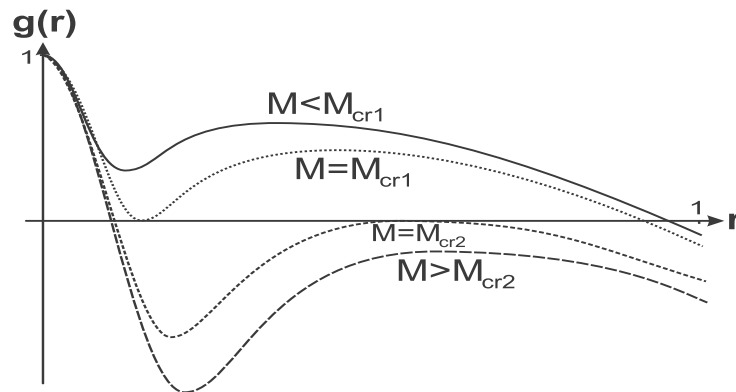
For two scales of vacuum density the geometry can have not more than two horizons [85], a black hole horizon r_b , a cosmological horizon r_c , and an internal horizon r_a which are shown in Figure 3.

Figure 3. Metric function $g(r)$ for a regular cosmological black hole with the de Sitter center.



Two horizons r_a and r_b coincide at a certain value of a mass parameter M_{cr1} . The mass M_{cr1} puts a lower limit on a black hole mass [68]. The extreme state $r_b = r_c$ puts an upper limit on a mass of a black hole M_{cr2} . Four configurations including two extreme states and two one-horizon configurations are shown in Figure 4.

Figure 4. Metric function $g(r)$ for space-time with the de Sitter center asymptotically de Sitter for $r \rightarrow \infty$.



Thermodynamics of a regular black hole with de Sitter interior is dictated by the typical behavior of the metric function $g(r)$, generic for the considered class of space-times specified by symmetry (9) of a stress-energy tensor satisfying the weak energy condition. A particular form of the density profile $\rho(r)$ affects only numerical values of thermodynamical parameters but not their dynamical behavior.

This paper is organized as follows. In Section 2 we present the basic features of space-time with de Sitter center in asymptotically de Sitter space. In Section 3 we analyze thermodynamics of horizons. In Section 4 we study evolution of a regular cosmological black hole during evaporation. In Section 5 we summarize the results.

We keep fixed an internal Λ (as corresponding to a certain fundamental symmetry scale [64,81]). We keep also fixed (following [16,18]) a background λ , so that the results are applicable to the case when a time scale of evaporation is less than a time scale of eventual changing λ .

2. Basic Features of Space-Time

The stress-energy tensor responsible for geometry (10) connects two de Sitter vacua: $T_{\mu\nu} = (8\pi G)^{-1}(\Lambda + \lambda)g_{\mu\nu}$, and $T_{\mu\nu} = (8\pi G)^{-1}\lambda g_{\mu\nu}$ at infinity. Its density component is given by

$$T_t^t(r) = \rho(r) + (8\pi G)^{-1}\lambda; \quad \rho(r) \rightarrow (8\pi G)^{-1}\Lambda \quad \text{as } r \rightarrow 0 \tag{11}$$

and includes a background vacuum density $\rho_\lambda = (8\pi G)^{-1}\lambda$ and the dynamical density ρ which should vanish at $r \rightarrow \infty$ quickly enough to ensure the finiteness of the mass

$$M = 4\pi \int_0^\infty \rho(r)r^2 dr \tag{12}$$

Space-time described by the metric function (10) has three characteristic length scales

$$r_g = 2GM; \quad r_0 = \sqrt{\frac{3}{\Lambda}}; \quad l = \sqrt{\frac{3}{\lambda}} \tag{13}$$

where l is related to the background vacuum density, $\rho_\lambda = (8\pi G)^{-1}\lambda$, and r_0 to the de Sitter vacuum density in the origin, $\rho_0 = (8\pi G)^{-1}\Lambda$. Normalizing r to r_0 or to l we get the characteristic parameter relating two vacuum scales, Λ and λ

$$q = \frac{l}{r_0} = \sqrt{\frac{\Lambda}{\lambda}} \tag{14}$$

For $r \gg r_*$ where

$$r_* = (r_0^2 r_g)^{1/3} \tag{15}$$

is the characteristic scale of space-times with the de Sitter interior [52,54], the metrics (10) are asymptotically Schwarzschild-de Sitter, Equation (2), or asymptotically Schwarzschild in the case $\lambda = 0$.

For $r \ll r_*$ the metric function is asymptotically de Sitter with $\Lambda + \lambda$.

A mass (12) for a regular cosmological black hole is confined within a certain range $M_{cr1} < M < M_{cr2}$ which depends on the parameter q [68].

For numerical calculations we adopt the density profile [54]

$$\rho(r) = \rho_0 e^{-r^3/r_0^2 r_g} \tag{16}$$

which describes the de Sitter-Schwarzschild transition in a simple semiclassical model for vacuum polarization in the spherically symmetric gravitational field [80]. Relevant physical mechanism can be self-regulation of geometry noted by Poisson and Israel [52]: An asymptotically flat space-time generated during spherically symmetric gravitational collapse can be described by the Schwarzschild vacuum solution down to the quantum barrier. Below this barrier there may exist a layer of an uncertain depth in which geometry could be self-regulatory and describable semiclassically by the Einstein field equations with a source term representing vacuum polarization effects [52]. In a gravitational collapse all fields contribute to vacuum polarization. Complexity of such a task is evident. However one can use the advantage of involving all of the fields in a collapse: all of them contribute, via Einstein equations, to gravitational field; a limiting density in a collapse could be achieved at the Planck or perhaps at the GUT scale and thus would depend on some unified coupling and would not depend on specific parameters of particular fields (the Schwarzschild black hole which represents the result of a collapse, depends only on mass parameter M). Therefore one can expect that the resulting effect would be vacuum polarization in a resulting gravitational field [54]. It can be evaluated qualitatively applying an intuitive semiclassical approach as described, e.g., by Novikov and Frolov [86]: in accordance with the uncertainty relation, the lifetime of a virtual pair of particles with energy mc^2 is $\tau \sim \hbar/mc^2$. In a time τ particles can move apart from each other at the distance $l_0 \sim \hbar/mc$. The probability w to find particles separated by a distance l is proportional to $\exp(-l/l_0)$. To create real particles with a charge g , a field F should produce work $gFl \sim mc^2$. As a result a vacuum polarization and particle creation effects in a field F are described by the Schwinger formula [86] $w \sim \exp(-\alpha m^2 c^3 / \hbar g F) \sim \exp(-F_{crit}/F)$, where α depends on detailed properties of a field F . In the case $F < F_{crit}$ this qualitative formula agrees with the results of detailed calculations for particular fields [86]. Gravitational field tension in the spherically symmetric case is characterized by the curvature component $F \sim r_g/r^3$, and the critical value for the case of self-regulation to a de Sitter core is related to the de Sitter curvature, $F_{crit} \sim r_0^{-2}$. As a result of this consideration [80] we get the density profile (16). It depends, via $r_0^2 = 3/\Lambda$, on a limiting density $\rho_0 = (8\pi G)^{-1}\Lambda$ which is related to a certain unification scale ($\rho_0 \propto M_{unif}^4$).

For the case of the density profile (16) the mass function is given by [54]

$$\mathcal{M}(r) = M \left(1 - e^{-r^3/r_0^2 r_g} \right) \tag{17}$$

In all pictures below we use the normalization $r \rightarrow r/l$ so that the mass parameter is normalized to l/G .

Horizon-mass diagram is plotted in Figure 5 with the the density profile (16). Dependence of boundary masses M_{cr1} and M_{cr2} on q is shown in Figure 6.

Figure 5. Horizons-mass diagram for $q = 50$.

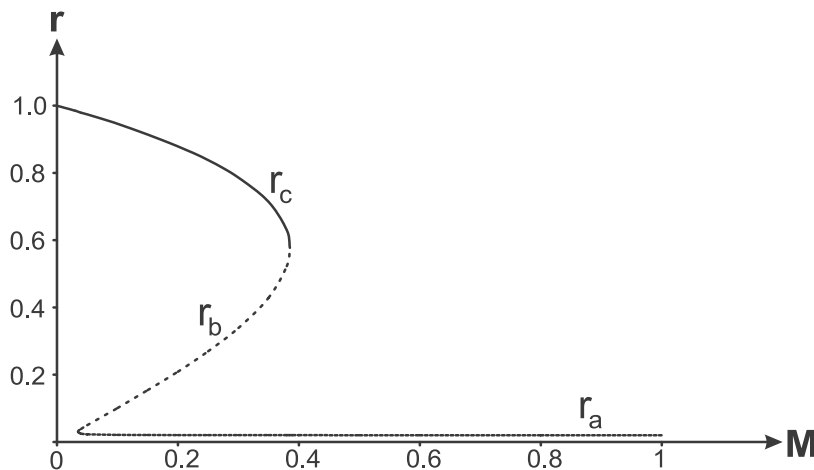
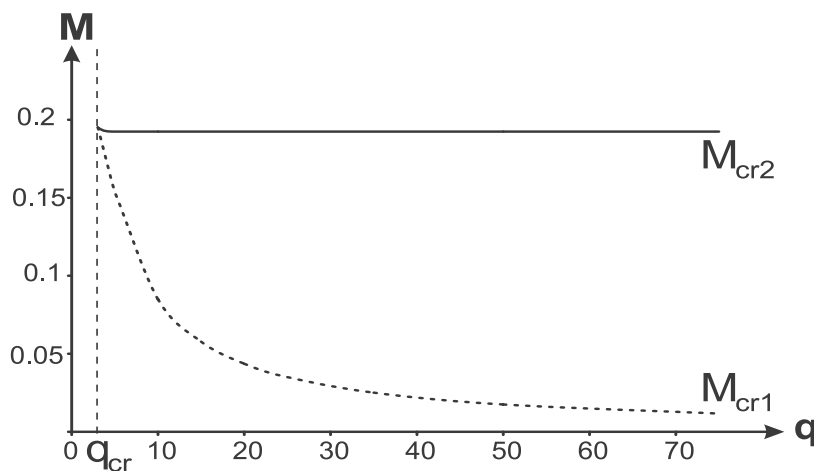


Figure 6. Critical masses dependently on q .



The point where two critical masses coincide, $q = q_{cr}$, corresponds to a triple horizon.

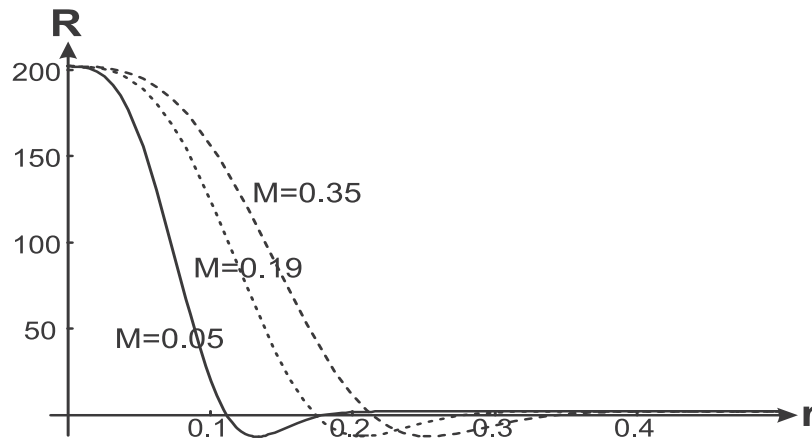
For any geometry with the de Sitter center there exist zero gravity surfaces defined by $p_{\perp}(r) = 0$ [64,80], beyond which the strong energy condition ($\rho + \sum p_k \geq 0$) is violated and gravitational attraction becomes gravitational repulsion.

For geometries satisfying the weak energy condition, there exist also surfaces of zero 4- and 3-scalar curvatures [80] which can be essential for details of evaporation dynamics [65,81]. In the case of two vacuum scales the 4-curvature scalar

$$\mathcal{R} = 8\pi G(4\rho + 4\rho_{\lambda} + r\rho') \tag{18}$$

can have two zero points (see Figure 7 where R is normalized to 2λ), because $\mathcal{R} \rightarrow 4(\Lambda + \lambda)$ as $r \rightarrow 0$ and $\mathcal{R} \rightarrow 4\lambda$ as $r \rightarrow \infty$.

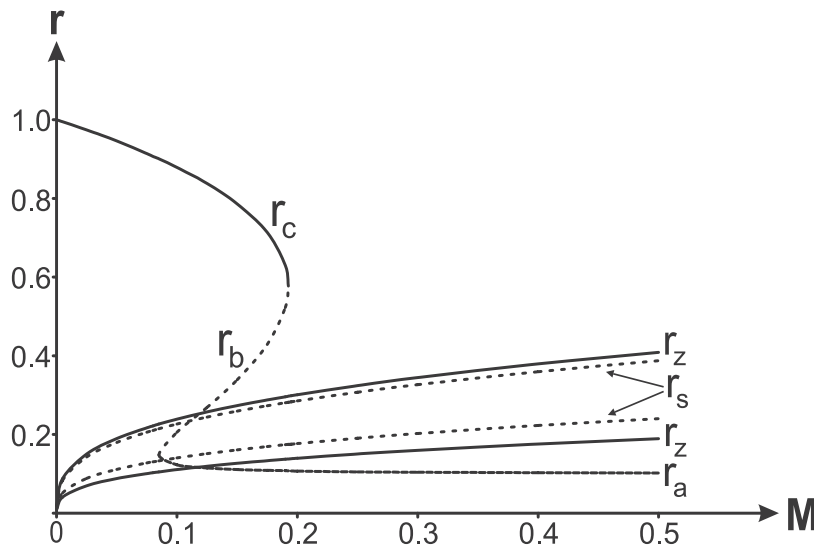
Figure 7. 4-curvature scalar for $q = 10$.



There exists a certain value of the parameter q , $q_R > q_{cr}$ such that $\mathcal{R}_{min} = 0$. For $q < q_R$, 4-curvature scalar is positive throughout the whole manifold. In the case of the density profile (16) $q_R = 3.71$.

Zero-gravity surfaces $r = r_z$ and surfaces of zero 4-curvature $r = r_s$ are plotted in Figure 8 together with the horizons for the case $q = 10$.

Figure 8. Horizons, zero gravity and zero 4-curvature surfaces for $q = 10$.



We see that there are two surfaces of zero curvature $r = r_s$ ($\mathcal{R}(r_s) = 0$), and two surfaces of zero gravity $r = r_z$ ($p_{\perp}(r_z) = 0$). In the case of two vacuum scales, the pressure p_{\perp} is negative near $r \rightarrow 0$ where $p_{\perp} = -(\rho_0 + \rho_{\lambda})$, and near $r \rightarrow \infty$ where $p_{\perp} = -\rho_{\lambda}$. All four characteristic surfaces fit between the internal horizon r_a and the black hole horizon r_b . During evaporation they change their mutual location [81], and this process can provide information about details of evaporation dynamics.

3. Thermodynamics of Horizons

Applying the Padmanabhan approach [12] we get on the horizons $r = r_h$

$$T_h = \frac{1}{4\pi} \left| \frac{1}{r_h} - \lambda r_h - 8\pi\rho(r_h)r_h \right|; \quad r_h = r_a, r_b, r_c \tag{19}$$

$$S_h = 4\pi r_h^2; \quad E_h = \frac{|g'|}{g} \frac{r_h}{2} = \frac{|g'|}{g} \left(\frac{A_h}{16\pi} \right)^{1/2}; \quad F_h = E_h - T_h S_h \quad (20)$$

A specific heat, $C_h = dE_h/dT_h$ is calculated from

$$C_h^{-1} = \frac{dT_h}{dr_h} \frac{dr_h}{dE_h} \quad (21)$$

which gives

$$C_h^{-1} = -\frac{1}{2\pi} \left[8\pi\rho'(r_h)r_h + 8\pi\rho(r_h) + \lambda + \frac{1}{r_h^2} \right] \quad (22)$$

It is easy to check that C_h^{-1} can be written as

$$C_h^{-1} = \frac{1}{2\pi} \left(\frac{g'(r_h)}{r_h} + g''(r_h) \right) \quad (23)$$

On a double horizon $r_h = r_d$ a specific heat takes the value [84]

$$C_d^{-1} = \frac{1}{2\pi} g''(r_d) \quad (24)$$

This simple formula is quite powerful since it tells us unambiguously that an extreme state with a double horizon is thermodynamically stable when it appears in a minimum of the metric function $g(r)$, and thermodynamically unstable when it appears in its maximum.

An observer in the R-region $r_b < r < r_c$ can detect radiation from the black hole horizon r_b and from the cosmological horizon r_c . An observer in the R-region $0 \leq r < r_a$ can detect radiation from the internal horizon r_a which is his cosmological horizon.

The question of stability of an internal horizon r_a can be essential, especially in the asymptotically flat case. In singular black hole space-times the internal Cauchy horizons suffer from blue shift instabilities. In the case of a black hole with de Sitter vacuum core one can expect stability of an internal horizon. General arguments are given in [87]: in a singular black hole an infinite blue shift of inward directed signals combined with infalling radiation leads to divergence of stress-energy tensor T_k^i near the Cauchy horizon and thus to its instability. In the regular case there exist a limiting density and limiting curvature, and the back reaction of matter does not allow unlimited growth of the curvature and an effective T_k^i . Achieving a limiting density is directly related to formation of the de Sitter core, and one may expect stability of the internal horizon [87]. Detailed investigation for the case of renormalization group improved black hole (without a de Sitter core) has shown that quantum gravity effects weaken the strength of the Cauchy singularity and suggest that presence of some self-regulation mechanism could prevent the local curvature from divergence on the Cauchy horizon [88].

Derivative of the metric function $g(r)$ is negative on the cosmological horizons and positive on a black hole horizon. As a results on the horizons $r_h = r_a, r_h = r_c$

$$T_{c,a} = \frac{1}{4\pi} \left(8\pi\rho(r_h)r_h + \frac{3r_h}{l^2} - \frac{1}{r_h} \right); \quad E_h = -\frac{r_h}{2} \quad (25)$$

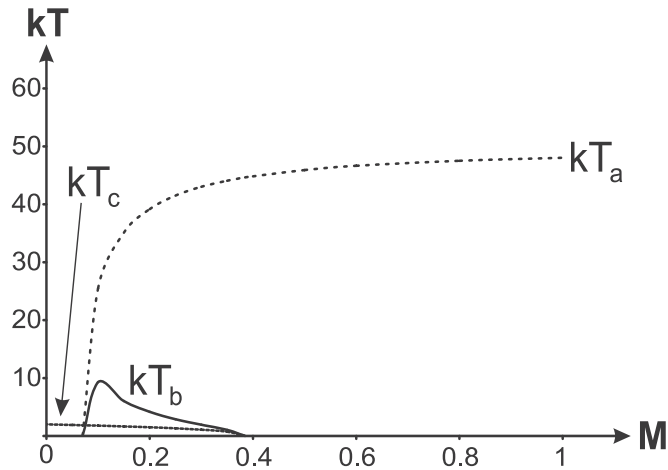
and on a black hole horizon $r_h = r_b$

$$T_b = \frac{1}{4\pi} \left(\frac{1}{r_b} - \frac{3r_b}{l^2} - 8\pi\rho(r_b)r_b \right); \quad E_b = \frac{r_b}{2} \quad (26)$$

Temperature-mass diagrams for all three horizons are shown in Figure 9. Numerical analysis shows that dependence of the temperature of the cosmological horizon on the mass M and on the horizon r_c is very similar for all $q > 5$.

In all the pictures below the temperature is normalized in such a way that $\hbar/4\pi c = 1$ and $k = 1$.

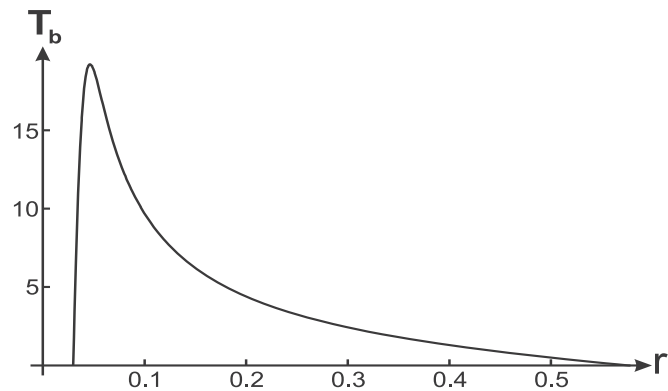
Figure 9. Temperatures in the case $q = 25$.



3.1. Thermodynamics of the Black Hole Horizon

Temperature on a black hole horizon is shown in Figure 10.

Figure 10. Dependence of T_b on r_b for the case $q = 50$.



This curve is generic and defined actually by the asymptotic behavior of the metric function $g(r)$ [84].

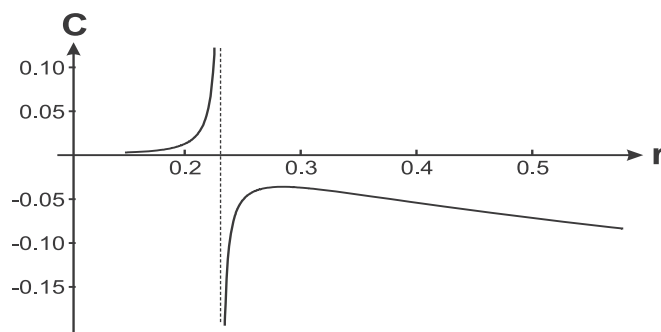
$T_b \rightarrow 0$ as $r_b \rightarrow r_c$ (zero surface gravity, $g'(r_b = r_c) = 0$)

$T_b \rightarrow 0$ as $r_a \rightarrow r_b$ (zero surface gravity, $g'(r_a = r_b) = 0$)

Hence it should exist a maximum in between. At the maximum a specific heat is broken and changes sign ($C_b = \frac{dE_b}{dT_b} = \frac{dE_b}{dr_b} \frac{dr_b}{dT_b} \rightarrow \infty$), hence a second order phase transition occurs during evaporation [80,84]. At this point the temperature T_b acquires its maximal value.

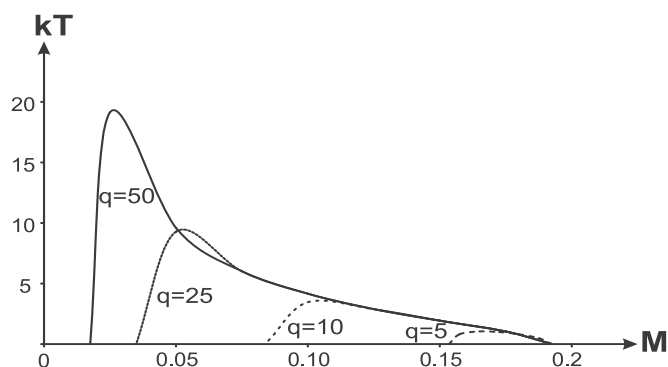
Behavior of a specific heat on the black hole horizon dependently on r_b is shown in Figure 11.

Figure 11. Dependence of C_b on r_b for the case $q = 10$.



Numerical analysis of specific heat did not reveal an essential differences in dependence of C_b on mass M and on the horizon radius r_b . Vanishing of temperature on a double horizon $r_a = r_b$ occurs at a certain value of the parameter $M_{cr1}(q)$, as we see in Figure 12.

Figure 12. Temperature on the black hole horizon.



Maximal temperature—temperature at the phase transition—is given by

$$T_{b \max} = -\frac{1}{4\pi} g''(r_b) r_b \tag{27}$$

For the case of the density profile (16)

$$T_{tr} \simeq 0.2 T_{Pl} \sqrt{\rho_0 / \rho_{Pl}} \tag{28}$$

For $\rho_0 = \rho_{GUT}$ and $M_{GUT} \simeq 10^{15} \text{ GeV}$

$$T_{tr} \simeq 0.2 \times 10^{11} \text{ GeV}$$

3.2. The Case of Global Temperature for an Observer between r_b and r_c

Let us now compare temperatures from a black hole and cosmological horizon because they can be measured by the same observer (pictured in Figure 13).

We compare these two temperatures in Figure 14. In general an observer in R-region $r_b < r < r_c$ would detect the mixture of radiations from his horizons. Their temperatures are shown in Figure 14.

Figure 13. R-region between the horizons r_b and r_c .

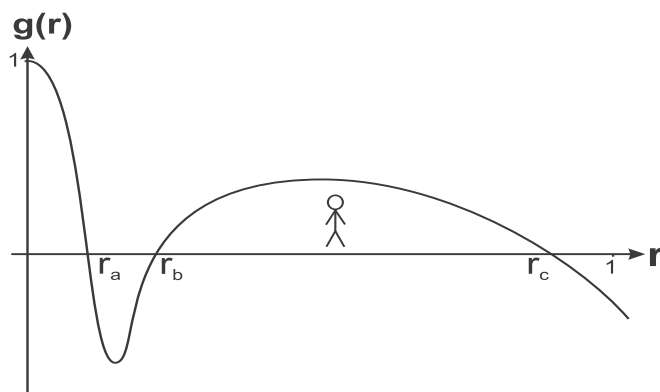
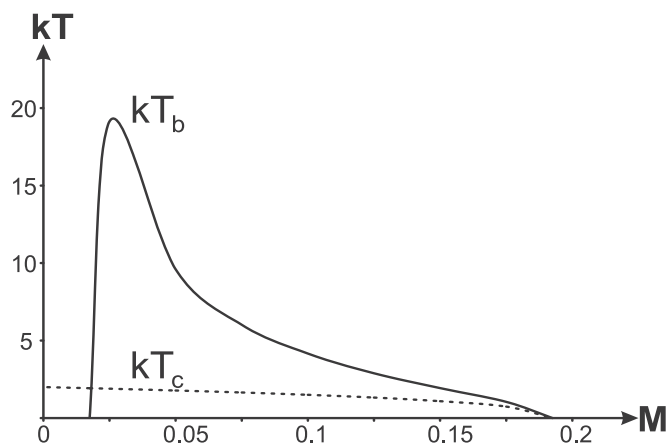
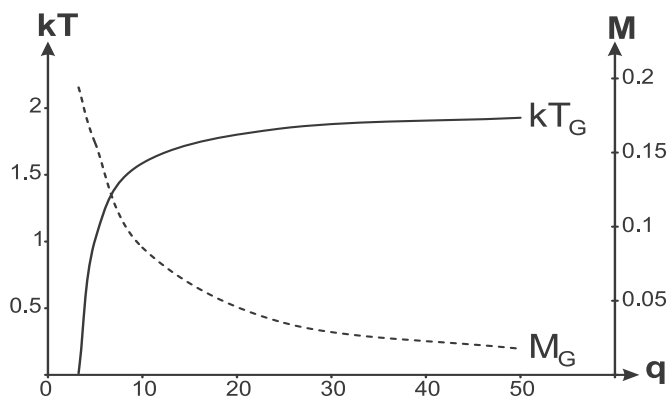


Figure 14. T_b and T_c for the case $q = 50$.



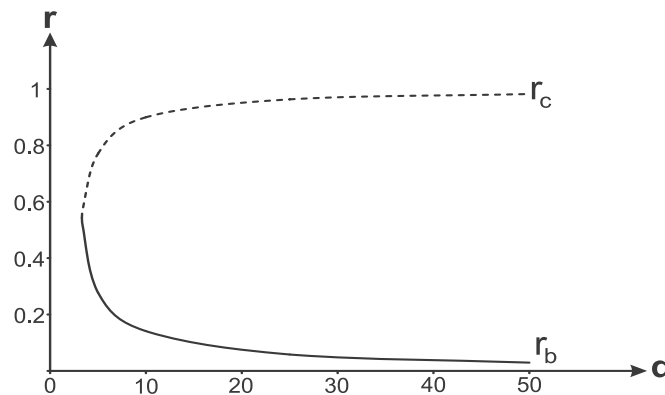
The most interesting possibility arising here is the existence of a certain range of masses for which temperatures on the black hole and cosmological horizons are equal, *i.e.*, the case when one can speak about a common (global) temperature for an observer in the R-region between the black hole horizon r_b and the cosmological horizon r_c . Dependence of the global temperature on the parameter q is shown in Figure 15, where we show also dependence of the mass M on q . It tells us that for each value of the mass parameter M there exists such a value of the parameter q that the relation of surface gravities on the black hole and cosmological horizons is a rational number.

Figure 15. Dependence of the global temperature kT_T and M_T on q .



Dependence of horizons on the parameter q in this case is shown in Figure 16.

Figure 16. Dependence of horizons on q in the case of existence of the global temperature.



Horizons coincides at $q = q_{cr}$, which corresponds to a triple horizon.

For a regular spherically symmetric space-time with $\Lambda > \lambda$ there exists a certain value q_{cr} at which, for a certain value M_{cr} , the metric function $g(r)$, its first and second derivative (and hence tangential pressure) vanish; as a result the temperature and the specific heat vanish, so the triple-horizon configuration is thermodynamically stable [84]. Near $q = q_{cr}$ a metric function has only one zero and a plateau distinguished by two conditions: $g' = 0, g'' = 0$. These two equations give two dependencies, $r_i(M)$ and $q_i(M)$. Imposing the third condition defining a horizon, $g = 0$, we define uniquely a triple-horizon configuration for any density profile [84].

For the case of the density profile (16) $q_{cr} = 3.24$. As we shall see below, the triple horizon is not involved in a black hole evolution during evaporation (see also [84]).

4. Evolution of a Black Hole During Evaporation

The main question is where move horizons?

For an observer in the R-region $0 \leq r \leq r_a$, the internal (for a black hole) horizon $r = r_a$ is his cosmological horizon, which is the boundary of his manifold, so that the second law of thermodynamics reads $dS_a \geq 0$. As a result, the evolution of r_a as governed by the second law gives $dr_a \geq 0$.

Looking at the horizon-mass diagram Figure 5 plotted for the density profile (16) we see that on the black hole horizon $dr_b/dM > 0$ while on both cosmological horizons $dr_h/dM < 0$:

$$\frac{dr_a}{dM} < 0; \quad \frac{dr_b}{dM} > 0; \quad \frac{dr_c}{dM} < 0 \tag{29}$$

It follows then that when r_a increases, mass M decreases by (29), hence black hole horizon shrinks, $dr_b < 0$, and cosmological horizon moves outward, $dr_c > 0$.

How general is the relation (29) and how it can be justified?

Following Teitelboim we can take derivative of the relation $g(r_h, M) = 0$ keeping λ constant [16]. In our case we keep constant also central Λ . It gives on the horizons

$$\frac{dr_h}{dM} = -\frac{\partial g}{\partial M} \frac{1}{g'} \tag{30}$$

With taking into account behavior of g' on the horizons, we should have

$$\frac{\partial g}{\partial M} < 0 \tag{31}$$

on each horizon in order to get (29).

Let us show that (31) holds everywhere (not only on the horizons) for the wide class of density profiles whose dependence on the coordinate r involves r/r^* where $r^* = (r_0^2 r_g)^{1/3}$ is the characteristic scale in a geometry with the de Sitter interior [52]. For the density profile

$$\rho(r) = \rho_0 \tilde{\rho}(r/r_*) \tag{32}$$

the mass function can be written as

$$\mathcal{M}(r) = 3M\phi(y); \quad \phi(y) = \int_0^y \tilde{\rho}(y)y^2 dy \tag{33}$$

where $y = r/r^*$.

The metric function takes the form

$$g = 1 - M^{2/3} \frac{1}{r_0^{2/3}} \left[\left(\frac{3}{2^{1/3}} \right) \frac{\phi(y)}{y} + \frac{(2^{2/3})}{q^2} y^2 \right] \tag{34}$$

It follows from (34) that in the considered case (31) holds everywhere. On the horizons we get

$$\frac{\partial g}{\partial M} = -\frac{2}{3M} \tag{35}$$

As a result, evolution goes towards a formation of the double horizon $r_a = r_b$.

Near the double horizon $r_b = r_c$ the specific heat C_b is negative by (24). The same relation requires C_b be positive near the double horizon $r_a = r_b$. Therefore it should occur the phase transition during evaporation where C_b is broken and changes sign and T_b acquires its maximal value (27).

Before the transition, $C_b < 0$, hence $dT_b/dr_b < 0$, when r_b decreases, E_b decreases too, temperature increases to a maximum (27) where C_b changes sign, so that after transition we have $dT_b/dr_b > 0$, and thus further decreasing r_b leads to decreasing T_b until it vanishes at the double horizon. At this point the specific heat C_b is positive and takes the value (24), free energy is positive and equal E_b , and energy E_b achieves its minimum, so that the configuration with the double horizon $r_b = r_a$ can be the thermodynamically stable endpoint of evolution during evaporation. Let us study now the evolution on the internal horizon. Its thermodynamical energy

$$E_a = -\frac{r_a}{2} \tag{36}$$

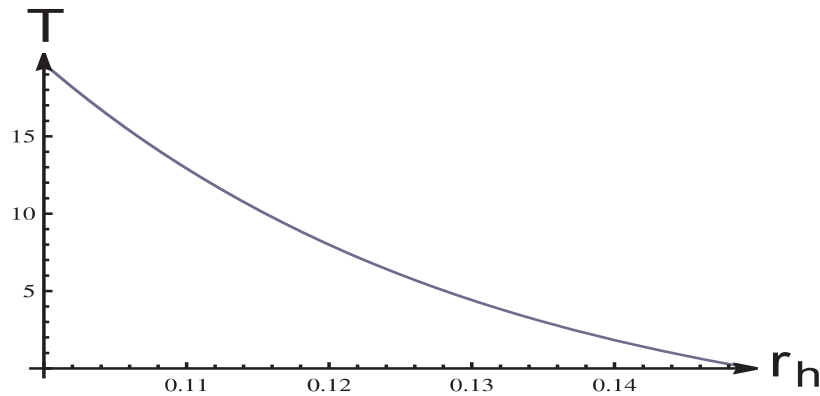
By (29), $dr_a/dM < 0$ and M decreases when r_a grows. Since $g' < 0$ on the internal horizon, we have

$$\frac{dT_a}{dr_a} = -\frac{T_a}{r_a} + \frac{1}{4\pi} g''(r_a) \tag{37}$$

Specific heat C_a is positive near $r_a \rightarrow r_b$, so that $dT_a/dE_a > 0$ and $dT_a/dr_a < 0$ when r_a approaches the double horizon. Hence T_a decreases with increasing r_a , the mass M decreases too, $dT_a/dM > 0$ and $dT_a/dr_a < 0$, so the growth in r_a leads to monotonic decreasing of the mass M and of the temperature T_a until it vanishes at the double horizon where the energy E_a achieves its minimum.

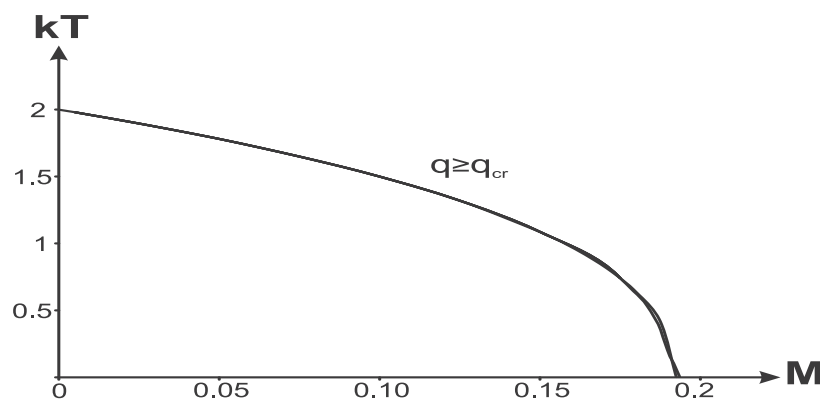
Temperature of the internal horizon is shown in Figure 17 for $q = 10$. It decreases monotonically with increasing r_a , and vanishes for $M = M_{cr1}$ when $r_a = r_b$.

Figure 17. Temperature on the internal horizon r_a .



The cosmological horizon r_c moves outwards during evaporation. The reasoning is similar to the case of r_a but the essential difference is that the specific heat is negative near the double horizon $r_b = r_c$. Hence $dT_c/dE_c < 0$ and $dT_c/dr_c > 0$; because the mass decreases by virtue of (29), $dT_c/dM < 0$ which we see in Figure 18. Starting from the double horizon $r_b = r_c$ evolution must thus occur as follows: M decreases and r_c increases by (29), hence E_c decreases, according to (25), and specific heat remains negative. Numerical analysis shows that for $q > q_{cr}$ the temperature on the cosmological horizon T_c is almost insensitive to the parameter q as we see in Figure 18.

Figure 18. Temperature on the cosmological horizon r_c .



We conclude that a regular cosmological black hole leaves behind the thermodynamically stable double-horizon remnant $M = M_{cr1}$ with zero temperature and positive specific heat.

Let us note that this conclusion follows unambiguously from thermodynamics of horizons, so that a regular cosmological black hole, like the asymptotically flat regular black hole [65,80], leaves behind the remnant free of the existential problems.

For the case of the density profile (16) mass of the remnant

$$M_{remnant} \simeq 0.3M_{Pl}\sqrt{\rho_{Pl}/\rho_0} \tag{38}$$

For $\rho_0 = \rho_{GUT}$ and $M_{GUT} \simeq 10^{15} \text{GeV}$

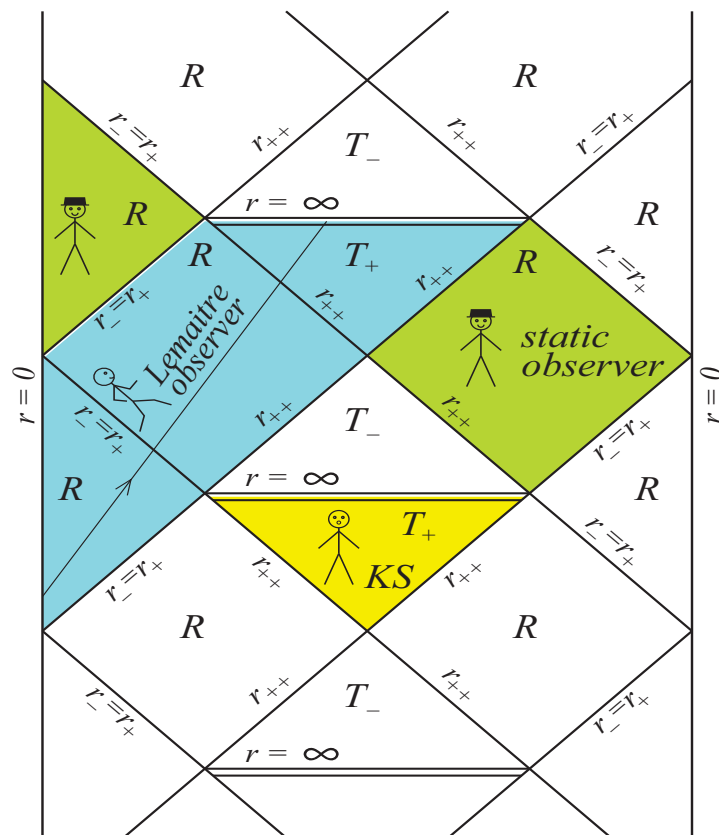
$$M_{remnant} \simeq 10^3 \text{g}$$

5. Summary and Discussion

We have studied thermodynamics of regular spherically symmetric cosmological black holes with two vacuum scales, Λ as $r \rightarrow 0$ as a certain fundamental symmetry scale, and the background $\lambda < \Lambda$. We applied the Padmanabhan approach relevant for the multi-horizon space-time with non-zero pressure. We present the basic thermodynamical formulae valid for any density profile satisfying the weak energy condition (needed for replacing a Schwarzschild singularity with a de Sitter vacuum interior).

Let us first discuss the question of entropy. The Padmanabhan obtains the same non-zero value for entropy of any horizon [12] as dictated by the Bekenstein formula for a black hole entropy [2]. Generalized uncertainty principle predicts zero entropy of the Planckian remnant in agreement with the third law of thermodynamics for a zero temperature thermodynamical system. The key point is that the entropy related to a horizon is the measure of a lack of information about a system surrounded by this horizon for an observer in a relevant R-region. The causal structure of space-time for a regular double-horizon remnant asymptotically de Sitter at both origin and infinity, is shown in Figure 19 [85,89].

Figure 19. Global structure of space-time for a double-horizon remnant in de Sitter space.



This picture shows how the manifold of events is seen by different observers. Here r_- is the internal horizon, r_+ is the black (white) hole horizon, and r_{++} is the cosmological horizon. Thermodynamics of

horizons is considered from the point of view of static observers in R-regions (observers in hats). Static observers are those who move on world lines of constant r , θ and ϕ which coincide with orbits of the static Killing vector $K = \partial/\partial t$ [9]. T-regions correspond to homogeneous anisotropic cosmological models of Kantowski-Sachs type [85,90]. Lemaitre observers (using coordinates, e.g., related to radial timelike geodesics) see two R-regions and one T-region.

The internal horizon r_- is the cosmological horizon for an observer in the R-region $0 \leq r < r_-$. For a static observer in this region boundaries of his manifold are horizons $r_- = r_+$ in his absolute past and future (his time coordinate changes from $t \rightarrow -\infty$ to $t \rightarrow +\infty$). Such an observer has no access to information beyond the horizons $r_- = r_+$. A static observer in the R-region $r_- = r_+ < r < r_{++}$ has no access to information beyond the horizon $r_+ = r_-$ and cosmological horizon r_{++} . In accordance with the causal structure of space-time, static observers feel the lack of information from regions beyond their horizons, and it seems evident that measure of this information cannot rather be zero, suggesting in particular a non-zero entropy for the remnants. It follows that the question of the remnant entropy, as well as the question of consensus between non-zero remnant entropy and third law of thermodynamics, needs further investigation.

We studied in details dynamics of all three horizons and found that dynamics of evaporation is dictated in essence by generic behavior of the regular metric with the de Sitter interior.

We found that in the case of a regular cosmological black hole there exists a certain range of parameters M and $q = \sqrt{\Lambda/\lambda}$, for which an observer in the region between the black hole horizon r_b and the cosmological horizon r_c would detect the global temperature.

During evaporation a second-order phase transition occurs where the specific heat on the black hole horizon is broken and changes its sign, and the black hole temperature achieves its maximum. At the final stage temperature drops to zero and a black hole evolves to soliton-like double-horizon remnant.

Soliton-like character of remnants was noted in [58,63,65,80]. The existence of gravitational solitons with the de Sitter interior was found first in [80] including those without a black hole horizon. They can arise not only as final products of evaporation but also in a way similar to primordial black hole formation from quantum fluctuations emerging in a quantum tunnelling process [67]. Cosmological production of positive mass noncommutative black holes and solitons was studied in [63] where it was shown that they would have plentifully been produced during inflationary epoch [63].

Let us emphasize that the basic features of evaporation dynamics of a regular black hole with the de Sitter interior are generic and dictated by generic behavior of a metric function $g(r)$ [80,84]. A particular form of the density profile $\rho(r)$ affects only numerical values of thermodynamical parameters but not their dynamical behavior [84]. The Hawking temperature drops to zero when an internal and black hole horizons coalesce just because the surface gravity $\kappa \propto g'(r)$ vanishes at an extremum of a metric function $g(r)$ [80]. In the asymptotically flat case it vanishes as M^{-1} in the Schwarzschild limit, hence a temperature-mass function must have a maximum (defined by g'') where the specific heat is broken and changes its sign which testifies for a second-order phase transition in the course of evaporation [80]. Similar behavior was found in [58,59] for the renormalization group improved black hole [88], in [62] for a noncommutative black hole, and in [82] for a minimal black hole model [83]—even though in [58,82] thermodynamical energy was identified with the black hole mass M which is true for the Schwarzschild black hole with one horizon but not true for a multihorizon spacetime with non-zero pressure [12]. This

mistake leads only to vanishing specific heat of the remnant but not affect the typical behavior—zero temperature of the remnant and the existence of the maximal temperature [58,62,80,82]. The proper choice of thermodynamical energy leads to the remnant with the positive specific heat [84]. For a cosmological regular black hole temperature drops to zero when black hole horizon coalesce with the cosmological horizon ($\kappa \propto g'$ vanishes in the maximum of $g(r)$), so that temperature vanishes on both boundaries of the R-region $r_b < r < r_c$, hence it achieves a certain maximum value (proportional to g'') [84]. The same behavior was found recently for a noncommutative black hole with positive mass and the gaussian density profile [63].

We conclude that a regular spherically symmetric black hole in de Sitter space leaves behind a thermodynamically stable double-horizon remnant with the positive specific heat and zero temperature [49,84]. Its stability to small perturbations is now under investigation, preliminary results suggest stability in a wide range of density profiles. We can thus expect that regular black holes and their remnants can contribute to dark matter black holes ([41,91] and references therein).

Acknowledgment

This work was supported by the Polish National Science Center through the grant 5828/B/H03/2011/40.

References and Notes

1. Bardeen, J.M.; Carter, B.; Hawking, S.W. The four laws of black hole mechanics. *Commun. Math. Phys.* **1973**, *31*, 161–170.
2. Bekenstein, J.D. Black holes and entropy. *Phys. Rev.* **1973**, *7*, 2333–2346.
3. Hawking, S.W. Black-hole evaporation. *Nature* **1974**, *248*, 30–31.
4. Hawking, S.W. Particle creation by black holes. *Commun. Math. Phys.* **1975**, *43*, 199–220.
5. Bekenstein, J.D. Generalized second law of thermodynamics in black hole physics. *Phys. Rev.* **1974**, *9*, 3292–3300.
6. Bekenstein, J.D. Statistical black-hole thermodynamics. *Phys. Rev.* **1975**, *12*, 3077–3085.
7. Hawking, S.W. Black holes and thermodynamics. *Phys. Rev.* **1976**, *13*, 191–197.
8. Wald, R.M. *Quantum Field Theory in Curved Space and Black Hole Thermodynamics*; University of Chicago Press: Chicago, IL, USA, 1994.
9. Gibbons, G.W.; Hawking, S.W. Cosmological event horizons, thermodynamics, and particle creation. *Phys. Rev. D* **1977**, *15*, 2738–2751.
10. Bousso, R. Positive vacuum energy and the N-bound. *JHEP* **2000**, *0108*, 038:1–038:23.
11. Bousso, R. Bekenstein bounds in de Sitter and flat space. *JHEP* **2001**, *0111*, 035:1–035:14.
12. Padmanabhan, T. Classical and quantum thermodynamics of horizons in spherically symmetric spacetimes. *Class. Quant. Grav.* **2002**, *19*, 5387–5408.
13. Padmanabhan, T. The holography of gravity encoded in a relation between entropy, horizon area and the action for gravity. *Gen. Rel. Grav.* **2002**, *34*, 2029–2035.
14. Choudhury, T.R.; Padmanabhan, T. Concept of temperature in multi-horizon spacetimes: Analysis of Schwarzschild-De Sitter metric. *Gen. Rel. Grav.* **2007**, *39*, 1789–1811.

15. Cai, R.G. Cardy-Verlinde formula and asymptotically de Sitter spaces. *Phys. Lett. B* **2002**, *525*, 331–336.
16. Teitelboim, C. Gravitational thermodynamics of Schwarzschild-de Sitter space. In *Strings and Gravity. Tying the Forces Together*. Proceedings of the 5th Francqui Colloquium on Strings and Gravity, Brussels, Belgium, 19–21 October 2001; De Boeck & Larcier: Brussels, Belgium, 2003.
17. Gomberoff, A.; Teitelboim, C. De Sitter black holes with either of the two horizons as a boundary. *Phys. Rev. D* **2003**, *67*, 104024:1–104024:7.
18. Aros, R. De Sitter thermodynamics: A glimpse into nonequilibrium. *Phys. Rev. D* **2008**, *77*, 104013:1–104013:7.
19. Riess, A.G.; Filippenko, A.V.; Challis, P.; Clocchiattia, A.; Diercks, A.; Garnavich, P.M.; Gilliland, R.L.; Hogan, C.J.; Iha, S.; Kirschner, R.P.; *et al.* Observational evidence from supernovae for an accelerating universe and a cosmological constant. *Astron. J.* **1998**, *116*, 1009–1038.
20. Riess, A.G.; Kirschner, R.P.; Schmidt, B.P.; Iha, S.; Challis, P.; Garnavich, P.M.; Esin, A.A.; Carpenter, C.; Grashins, R.; *et al.* BV RI light curves for 22 type Ia supernovae. *Astron. J.* **1999**, *117*, 707–724.
21. Perlmutter, S.; Aldering, G.; Goldhaber, G.; Knop, R.A.; Nugent, P.; Castro, P.G.; Deustua, S.; Fabbro, S.; Goobar, A.; Groom, D.E.; *et al.* Measurements of Ω and Λ from 42 high-redshift supernovae. *Astrophys. J.* **1999**, *517*, 565–586.
22. Bahcall, N.A.; Ostriker, J.P.; Perlmutter, S.; Steinhardt, P.J. The cosmic triangle: Revealing the state of the universe. *Science* **1999**, *284*, 1481–1488.
23. Wang, L.; Caldwell, R.R.; Ostriker, J.P.; Steinhardt, P.J. Cosmic concordance and quintessence. *Astrophys. J.* **2000**, *530*, 17–35.
24. Spergel D.N.; Verde, L.; Peiris, H.V.; Komatsu, E.; Nolte, M.R.; Bennett, C.L.; Halpern, M.; Hinshaw, G.; Jarosik, N.; Kogut, A.; *et al.* First-year Wilkinson Microwave Anisotropy Probe (WMAP) observations: Determination of cosmological parameters. *Astrophys. J. Suppl. Ser.* **2003**, *148*, 175–194.
25. Schubnell, M. Probing dark energy in the accelerating universe with SNAP. In Proceedings of 8th Conference on the Intersections of Particle and Nuclear Physics (CIPANP 2003), New York, NY, USA, 19–24 May 2003; Parsa, Z., Ed.; AIP: New York, NY, USA, 2004; pp. 323–327.
26. Corasaniti, P.S.; Copeland, E.J. Constraining the quintessence equation of state with SnIa data and CMB peaks. *Phys. Rev. D* **2002**, *65*, 043004:1–043004:5.
27. Corasaniti, P.S.; Kunz, M.; Parkinson, D.; Copeland, E.J.; Bassett, B.A. Foundations of observing dark energy dynamics with the Wilkinson Microwave Anisotropy Probe. *Phys. Rev. D* **2004**, *70*, 083006:1–083006:15.
28. Hannestad, S.; Mortsell, E. Probing the dark side: Constraints on the dark energy equation of state from CMB, large scale structure, and type Ia supernovae. *Phys. Rev. D* **2002**, *66*, 063508:1–063508:5.
29. Tonry, J.L.; Schmidt, B.P.; Barris, B.; Candia, P.; Challis, P.; Clocchiatti, A.; Cail, A.L.; Filippenko, A.V.; Garnavich, P.; Hogan, C.; *et al.* Cosmological results from high- z supernovae. *Astrophys. J.* **2003**, *594*, 1–24.

30. Ellis, J. Dark matter and dark energy: Summary and future directions. *Phil. Trans. A* **2003**, *361*, 2607–2627.
31. Copeland, E.J.; Sami, M.; Tsujikawa, S. Dynamics of dark energy. *Int. J. Mod. Phys. D* **2006**, *15*, 1753–1935.
32. Copeland E.J. Models of dark energy. In Proceedings of the Invisible Universe International Conference, Paris, France, 29 June–3 July 2009; AIP: New York, NY, USA, 2010; pp. 132–138.
33. Strominger, A. The dS/CFT correspondence. *JHEP* **2001**, *0110*, 034:1–034:18.
34. Strominger, A. Inflation and the dS/CFT correspondence. *JHEP* **2001**, *0111*, 049:1–049:6.
35. MacGibbon, J.H. Can Planck-mass relics of evaporating black holes close the Universe? *Nature* **1987**, *329*, 308–309.
36. Rajagopal, K.; Turner, M.S.; Wilczek, F. Cosmological implications of axinos. *Nucl. Phys. B* **1991**, *358*, 447–470.
37. Carr, B.J.; Gilbert, J.H.; Lidsey, J.E. Black hole relics and inflation: Limits on blue perturbation spectra. *Phys. Rev. D* **1994**, *50*, 4853–4867.
38. Adler, R.J.; Chen, P.; Santiago, D. The generalized uncertainty principle and black hole remnants. *Gen. Rel. Grav.* **2001**, *33*, 2101–2108.
39. Chen, P.; Adler, R.J. Black hole remnants and dark matter. *Nucl. Phys. B* **2003**, *124*, 103–106.
40. Carr, B.J. Primordial black holes—Recent developments. Presented at the 22nd Texas Symposium on Relativistic Astrophysics, Stanford, CA, USA, 13–17 December 2004; No. 0204.
41. Nozari, K.; Mehdipour, S.H. Gravitational uncertainty and black hole remnants. *Mod. Phys. Lett. A* **2005**, *20*, 2937–2948.
42. Koch, B.; Bleicher M.; Hossenfelder S. Black hole remnants at the LHC. *JHEP* **2005**, *2005*, 053:1–053:20.
43. Nayak, G.C. Dark matter production at the LHC from black hole remnants. *Physics of Particles and Nuclei Letters* **2011**, *4*, 564–572.
44. Susskind, L. The World as a hologram. *J. Math. Phys.* **1995**, *36*, 6377–6396.
45. Lin, F.L. Black hole in de Sitter space. Presented at the International Symposium on Particles, Strings and Cosmology PASCOS 98, Boston, MA, USA, 22–29 March 1998.
46. Kin, F.K.; Soo, C. Quantum field theory with and without conical singularities: Black holes with a cosmological constant and the multi-horizon scenario. *Class. Quant. Grav.* **1999**, *16*, 551–562.
47. Bousso R.; Hawking, S.W. (Anti-)evaporation of Schwarzschild-de Sitter black holes. *Phys. Rev. D* **1998**, *57*, 2436–2442.
48. Huang, Q.G.; Ke, K.; Li, M. One conjecture and two observations on de Sitter space. *JHEP* **2006**, *2006*, 045:1–045:10.
49. Dymnikova, I. Regular black hole remnants. In Proceedings of the Invisible Universe International Conference, Paris, France, 29 June–3 July 2009; AIP: New York, NY, USA, 2010.
50. Sakharov, A.D. Expanding universe and the appearance of a nonuniform distribution of matter. *Sov. Phys. JETP* **1966**, *22*, 241–249.
51. Gliner, E.B. Algebraic properties of the energy-momentum tensor and vacuum-like states of matter. *Sov. Phys. JETP* **1966**, *22*, 378–383.

52. Poisson, E.; Israel, W. Structure of the black hole nucleus. *Class. Quant. Grav.* **1988**, *5*, L201–L205.
53. Dymnikova, I. Nonsingular spherically symmetric black hole. *Centrum Astronomiczne im. Mikolaja Kopernika* **1990**, *CAMK preprint 216*, pp. 1–9.
54. Dymnikova, I. Vacuum nonsingular black hole. *Gen. Rel. Grav.* **1992**, *24*, 235–242.
55. Perez, A. Spin foam models for quantum gravity. *Class. Quant. Grav.* **2003**, *20*, R43–R104.
56. Rovelli, C. *Quantum Gravity*; Cambridge University Press: Cambridge, UK, 2004.
57. Modesto, L. Loop quantum gravity and black hole singularity. Presented at the 17th SIGRAV Conference on General Relativity and Gravitational Physics, Turin, Italy, 4–7 September 2006.
58. Bonanno, A.; Reuter, M. Renormalization group improved black hole spacetimes. *Phys. Rev. D* **2000**, *62*, 043008–043032.
59. Bonanno, A.; Reuter, M. Spacetime structure of an evaporating black hole in quantum gravity. *Phys. Rev. D* **2006**, *73*, 083005–083017.
60. Nicolini, P. Noncommutative black holes, the final appeal to quantum gravity: A review. *Int. J. Mod. Phys. A* **2009**, *24*, 1229–1308.
61. Banerjee, R.; Gangopadhyay, S.; Modak, S.K. Voros product, noncommutative black hole and corrected area law. *Phys. Lett. B* **2010**, *686*, 181–187.
62. Nicolini, P.; Smailagic, A.; Spalucci, E. Noncommutative geometry inspired Schwarzschild black hole. *Phys. Lett. B* **2006**, *632*, 547–551.
63. Mann, R.B.; Nicolini, P. Cosmological production of noncommutative black hole. *arXiv* **2011**, arXiv: 1102.5096 [gr-qc].
64. Dymnikova, I. The algebraic structure of a cosmological term in spherically symmetric solutions. *Phys. Lett. B* **2000**, *472*, 33–38.
65. Dymnikova, I. The cosmological term as a source of mass. *Class. Quant. Grav.* **2002**, *19*, 725–740.
66. Dymnikova, I. Spherically symmetric space-time with regular de Sitter center. *Int. J. Mod. Phys. D* **2003**, *12*, 1015–1034.
67. Dymnikova, I.; Galaktionov, E. Vacuum dark fluid. *Phys. Lett. B* **2007**, *645*, 358–364.
68. Dymnikova, I.; Soltyssek, B. Spherically symmetric space-time with two cosmological constants. *Gen. Rel. Grav.* **1998**, *30*, 1775–1793.
69. Dymnikova, I.; Soltyssek, B. Nonsingular cosmological black hole. In *Particles, Fields and Gravitation*; Rembielinsky, J., Ed.; AIP: New York, NY, USA, 1998; pp. 460–471.
70. Dymnikova, I. Possibilities and surprises of vacuum dark fluid. *Gravitation and Cosmology* **2011**, *17*, 185–189.
71. Dymnikova, I.; Galaktionov, E. Dark ingredients in one drop. *Cent. Eur. J. Phys.* **2011**, *9*, 644–653.
72. It is invariant under radial Lorentz boosts which makes impossible to single out a preferred comoving reference frame and thus to fix the velocity with respect to a medium specified by $T_t^t = T_r^r$ —which is the intrinsic property of a vacuum, according to general heuristic definition of a vacuum given in [92].

73. Dymnikova, I. Variable cosmological term—Geometry and physics. In *Woprosy Matematicheskoy Fiziki i Prikladnoj Matematiki*; Tropp, A., Ed.; A.F. Ioffe Physico-Technical Institute: St. Petersburg, Russia, 2000; pp. 29–71, gr-qc/0010016.
74. Dymnikova, I. From vacuum nonsingular black hole to variable cosmological constant. *Gravitation and Cosmology Supplement* **2002**, *8*, 131–147.
75. Dymnikova, I. Self-gravitating spherically symmetric vacuum. In *General Relativity, Cosmology and Gravitational Lensing*; Marmo, G., Rubano, C., Scudellaro, P., Eds.; Bibliopolis: Napoli, Italy, 2002; pp. 95–129.
76. Dymnikova, I. Variable cosmological term. In *Cosmology and Gravitation*; Novello, M., Bergliaffa, S.E.P., Eds.; AIP: Melville, NY, USA, 2003; pp. 204–225.
77. Dymnikova, I. Cosmological term, mass and space-time symmetries. In *Beyond the Desert 2003*. Proceedings of the Fourth Tegernsee International Conference on Particle Physics Beyond the Standard BEYOND 2003, Castle Ringberg, Tegernsee, Germany, 9–14 June 2003; Klapdor-Kleinhaus, H.V., Ed.; Springer Verlag: Berlin, Germany, 2004; pp. 485–502, hep-th/0310047.
78. Dymnikova, I.; Galaktionov, E. Stability of a vacuum non-singular black hole. *Class. Quant. Grav.* **2005**, *22*, 2331–2358.
79. Dymnikova, I. Space-time symmetry and mass of a lepton. Presented at the 5th International Symposium on Quantum Theory and Symmetries, Valladolid, Spain, 22–28 July 2007. *J. Phys. A* **2008**, *41*, 304033–304052.
80. Dymnikova, I. De Sitter-Schwarzschild black hole: Its particlelike core and thermodynamical properties. *Int. J. Mod. Phys. D* **1996**, *5*, 529–540.
81. Dymnikova, I. Internal structure of nonsingular spherical black holes. In *Internal Structure of Black Holes and Spacetime Singularities*; Burko, L.M., Ori, A., Eds.; IOP: London, UK, 1997; pp. 422–438.
82. Myung, Y.S.; Kim, Y.W.; Park, Y.J. Black hole thermodynamics with generalized uncertainty principle. *Phys. Lett. B* **2007**, *645*, 393–397.
83. Hayward, S.A. Formation and evaporation of nonsingular black holes. *Phys. Rev. Lett.* **2006**, *96*, 031103:1–031103:4.
84. Dymnikova, I.; Korpusik, M. Regular black hole remnants in de Sitter space. *Phys. Lett. B* **2010**, *685*, 12–18.
85. Bronnikov, K.A.; Dobosz, A.; Dymnikova, I. Nonsingular vacuum cosmologies with a variable cosmological term. *Class. Quant. Grav.* **2003**, *20*, 3797–3814.
86. Novikov, I.D.; Frolov, V.P. *Physics of Black Holes*; Kluwer Acad. Publ.: Dordrecht, The Netherlands, 1989; Ch.9.
87. Frolov, V.P.; Markov, M.A.; Mukhanov, V.F. Black holes as possible sources of closed and semiclosed worlds. *Phys. Rev. D* **1990**, *41*, 383–394.
88. Bonanno, A.; Reuter, M. Quantum gravity effects near the null black hole singularity. *Phys. Rev. D* **1999**, *60*, 084011–084018.

89. Dymnikova, I. Λ^{μ}_{ν} geometries from the point of view of different observers. In *Beyond the Desert 2003*. Proceedings of the Fourth Tegernsee International Conference on Particle Physics Beyond the Standard BEYOND 2003, Castle Ringberg, Tegernsee, Germany, 9–14 June 2003; Klapdor-Kleinhaus, H.V., Ed.; Springer Verlag: Berlin, Germany, 2004; pp. 521–539, gr-qc/03100314.
90. Bronnikov, K.; Dymnikova, I. Regular homogeneous T-models with vacuum dark fluid. *Class. Quant. Grav.* **2007**, *24*, 5803–5816.
91. Frampton, P.H. High longevity microlensing events and dark matter black holes. Presented at the 11th conference on cosmology COSMO 08, Madison, WI, USA, 25–29 August 2008.
92. Landau, L.D.; Lifshitz, E.M. *Classical Theory of Fields*, 4th ed.; Butterworth-Heinemann: Oxford, UK, 1975.

© 2011 by the authors; licensee MDPI, Basel, Switzerland. This article is an open access article distributed under the terms and conditions of the Creative Commons Attribution license (<http://creativecommons.org/licenses/by/3.0/>.)